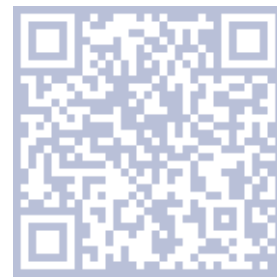


Retrieval of snow layer and melt pond properties from airborne imaging spectrometer observations

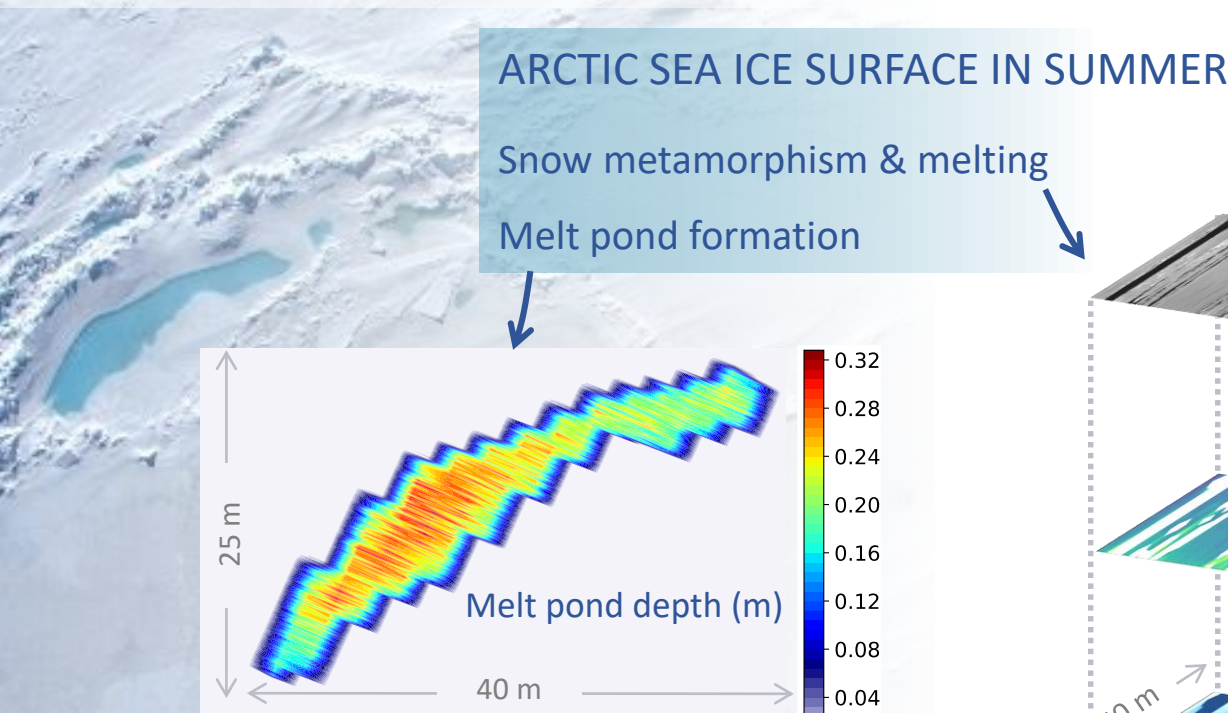
HS6.6
PICO4.9



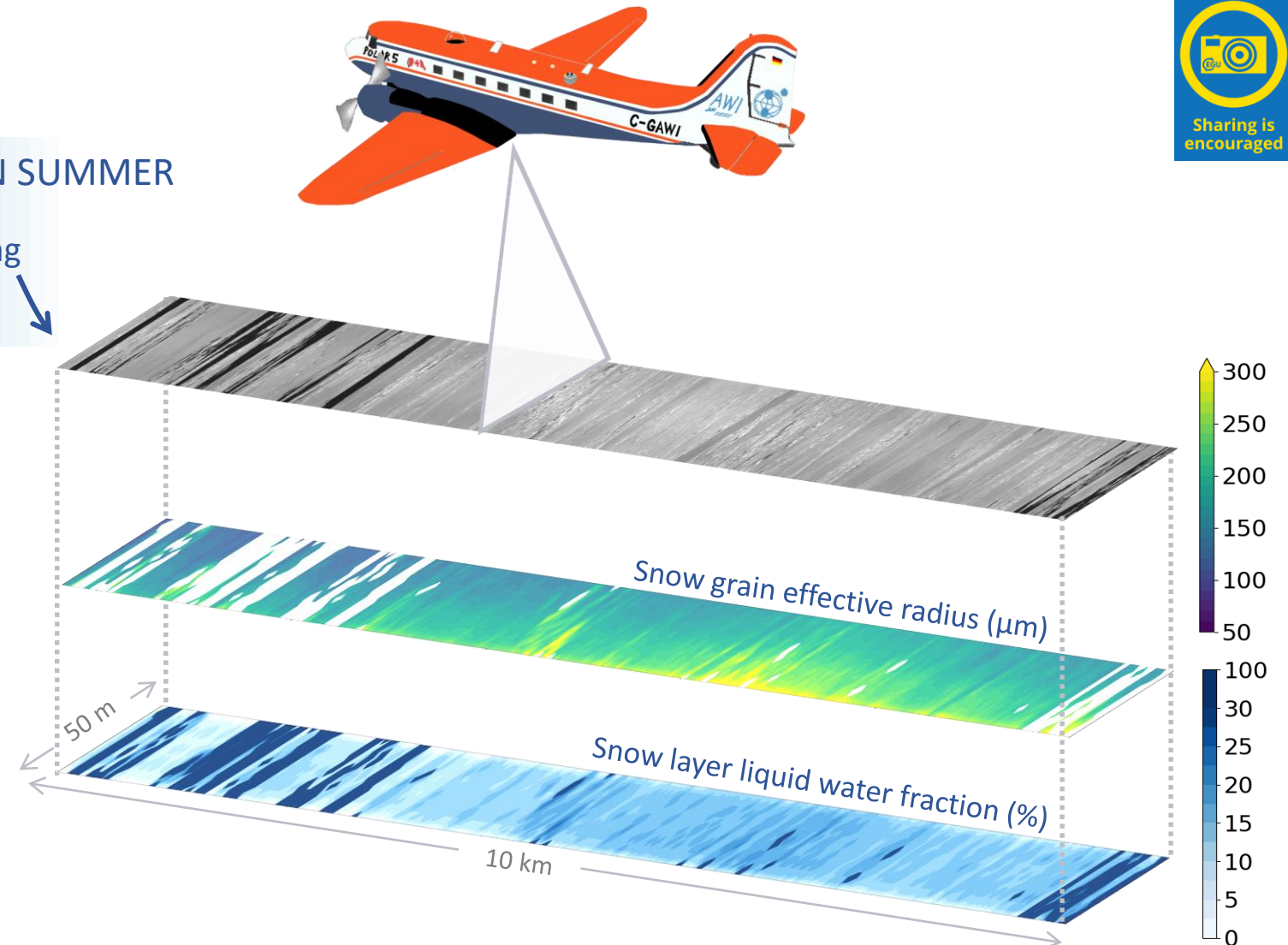
Sophie Rosenburg^{1*}, Charlotte Lange^{1*}, Evelyn Jäkel¹,
Michael Schäfer¹, André Ehrlich¹, and Manfred Wendisch¹

¹ Leipzig Institute for Meteorology (LIM), Leipzig University

*These authors contributed equally to this work.



UNIVERSITÄT
LEIPZIG



Retrieval of snow layer and melt pond properties from airborne imaging spectrometer observations



OVERVIEW

- Motivation and basics
- Measurements
- Retrieval of snow layer properties
- Retrieval of melt pond depth
- Potential uncertainty sources
- Conclusion

Click me for navigation



Abstract

NAVIGATION

previous

next

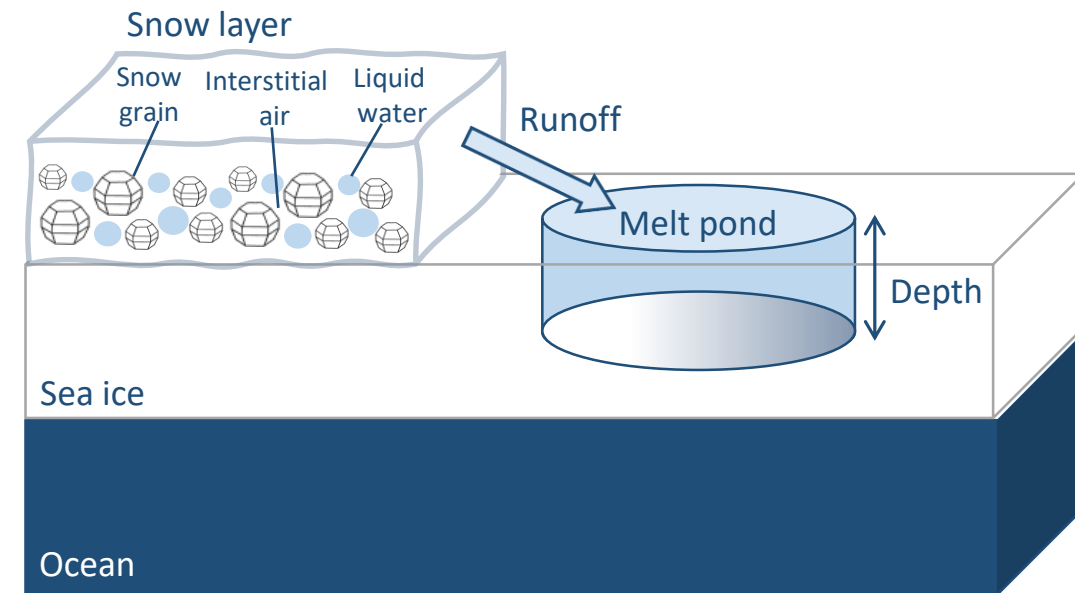
first
slide



Motivation and basics

Arctic surface albedo decrease
with melting progress

I. SNOW MELTING



II. PONDING

MEASUREMENT

Reflectance

$$\mathcal{R}_\lambda = \frac{\pi \cdot I_\lambda^\uparrow}{F_\lambda^\downarrow} \text{ sr}$$

upward radiance I_λ^\uparrow ($\text{W m}^{-2} \text{ nm}^{-1} \text{ sr}^{-1}$)

downward irradiance F_λ^\downarrow ($\text{W m}^{-2} \text{ nm}^{-1}$)

RETRIEVAL

Snow layer
liquid water fraction

$$f_{\text{LW}} = \frac{\text{LWC}}{\text{TWC}}$$

liquid water content LWC (g m^{-3})
total water content TWC (g m^{-3})

Effective
snow grain radius

$$r_{\text{eff}} = \frac{3 \int_{L_{\min}}^{L_{\max}} V(L) \cdot n(L) \, dL}{4 \int_{L_{\min}}^{L_{\max}} A(L) \cdot n(L) \, dL}$$

gamma size distribution n
max. dimension L (m)
effective area A (m^2)
and volume V (m^3)

Melt pond depth

Z (m)

Measurements



Arctic CLOUD Observations Using airborne measurements during polar Day (ACLOUD)^{1,2}

23 May – 26 June 2017

Research aircraft Polar 5 (AWI)³



- Upward radiance

Spectral imaging spectrometers

AisaEagle $\lambda = 400 - 990$ nm

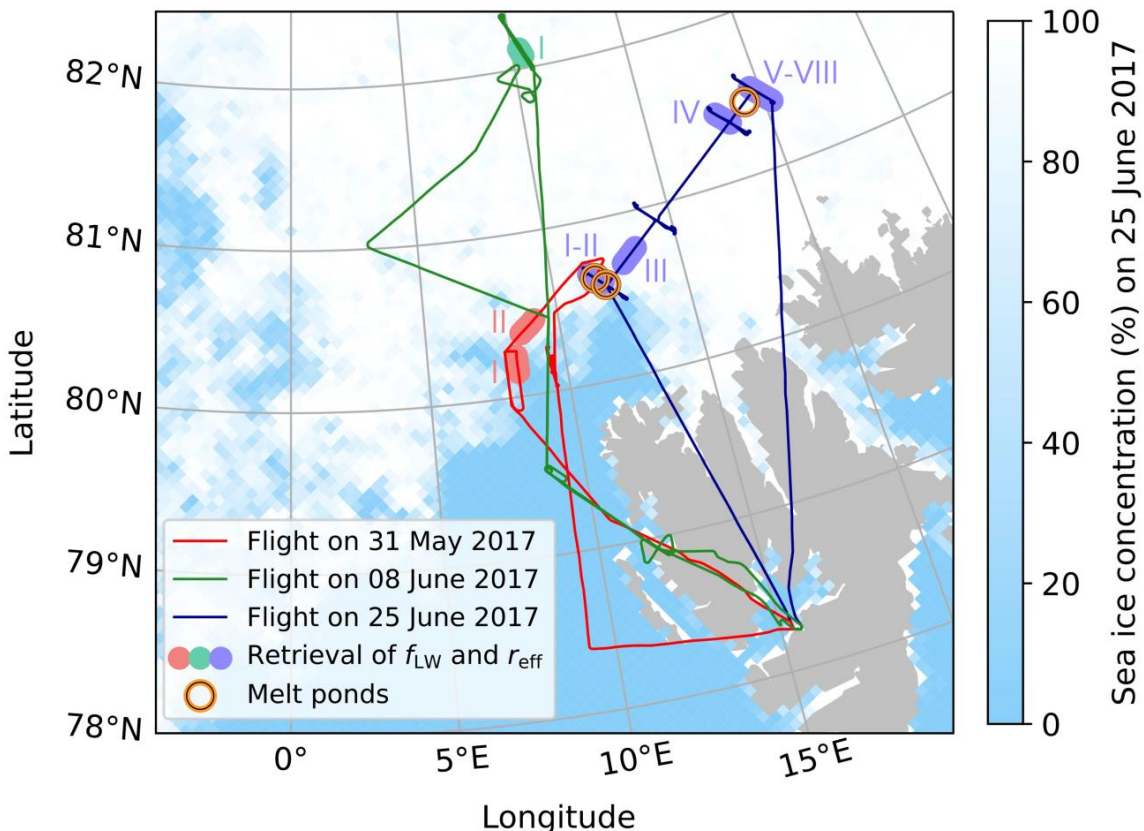
AisaHawk $\lambda = 940 - 2500$ nm

- Downward irradiance

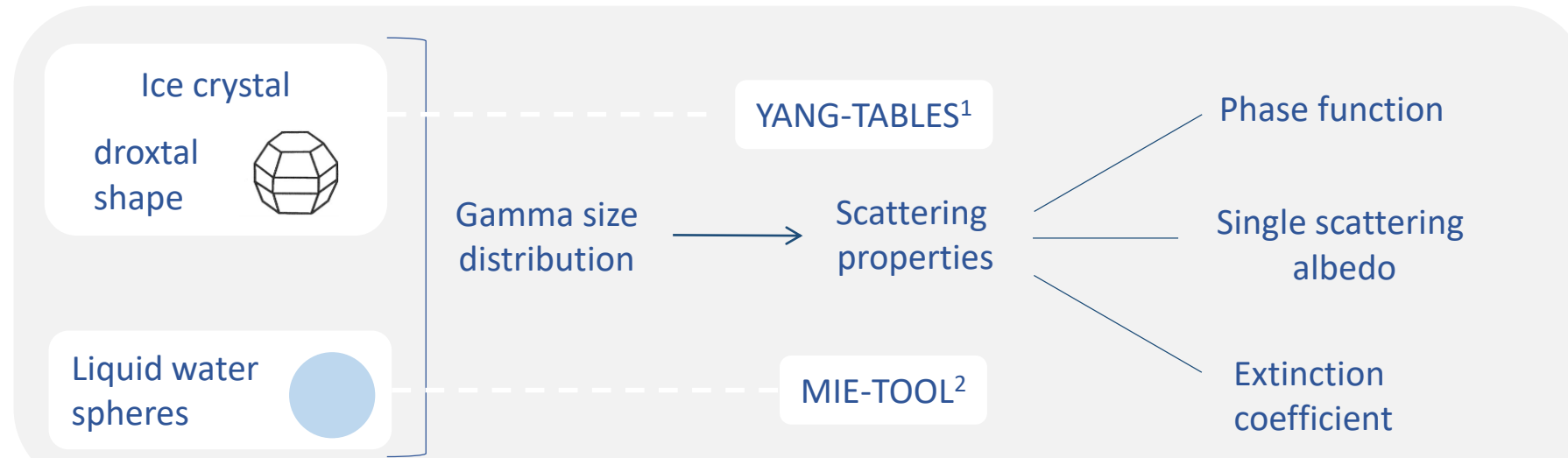
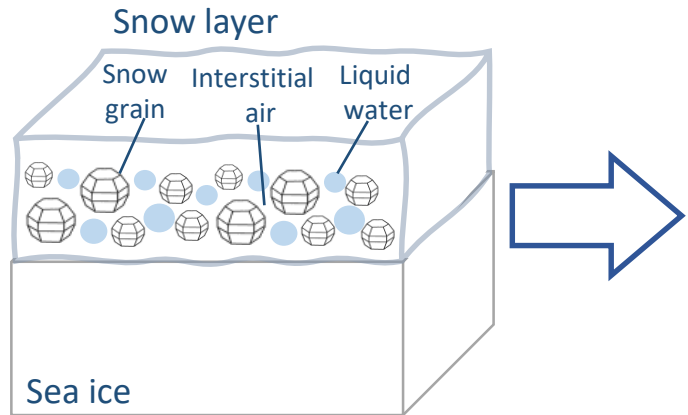
SMART albedometer $\lambda = 400 - 2150$ nm

→ Only cloud-free atmospheric conditions regarded to simplify radiative transfer simulations and retrievals

Highlighted retrieval areas along 3 flight tracks



¹Wendisch et al. (2019), ²Ehrlich et al. (2019), ³Wesche et al. (2016)



Simulation of snow layer reflectance spectra with *libRadtran*^{2,3}

with $r_{\text{eff}} = 50 - 800 \mu\text{m}$ (step: 50 μm)

$f_{\text{LW}} = 0 - 30 \%$ (step: 2.5 %)

for

selected flight sections

- Aircraft altitude & heading
- Solar azimuth & zenith angle
- Radiosonde profiles

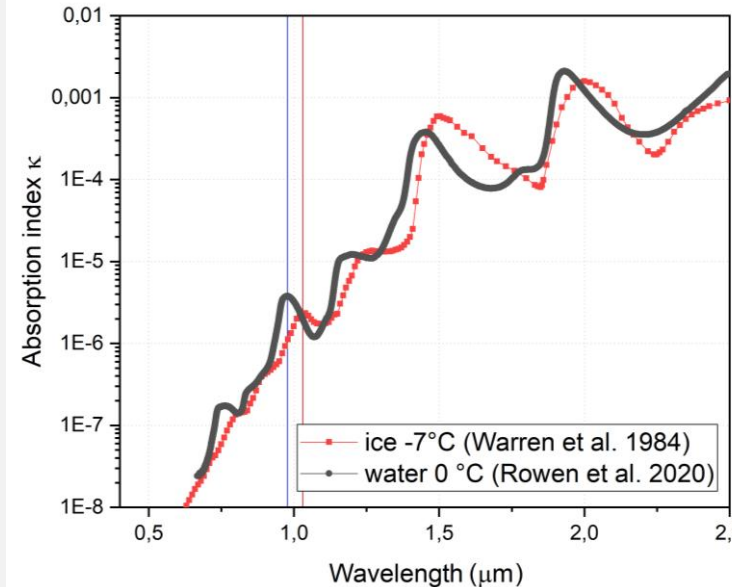
} temporally averaged

¹Yang et al. (2000), ²Mayer et al. (2019), ³Emde et al. (2016)

Retrieval of snow layer properties

THEORY

Spectrally shifted absorption maxima of liquid water and ice



Snow layer reflectance spectrum sensitive to
 Liquid water fraction f_{LW}
 Effective radius r_{eff}

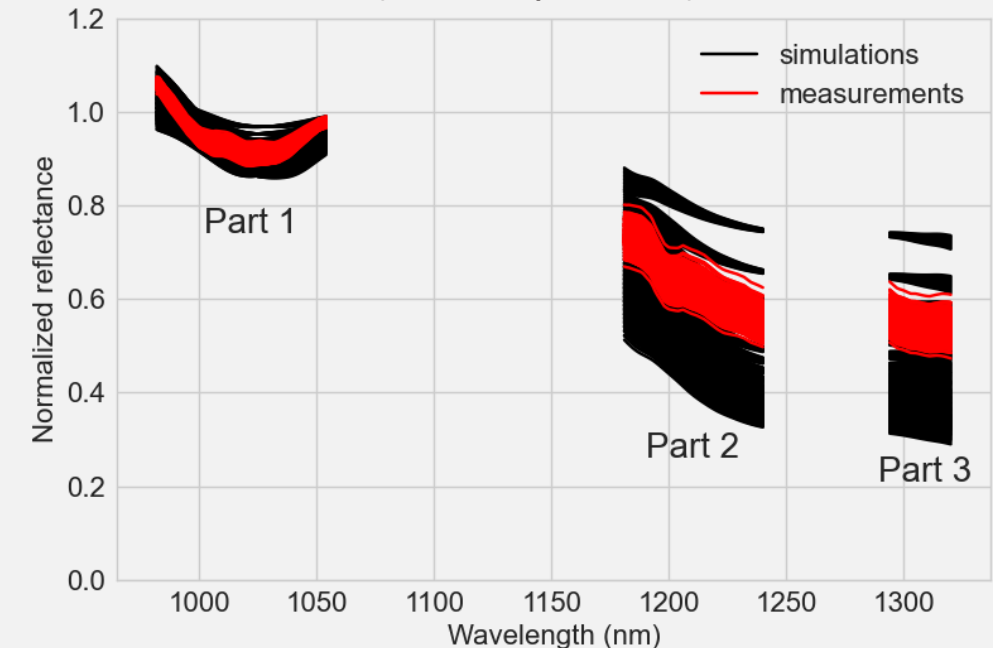
APPROACH

Simulations (*libRadtran*)

Snow layer reflectance spectra for varying f_{LW} and r_{eff}

Airborne measurements

COMPARISON (Least square fit)

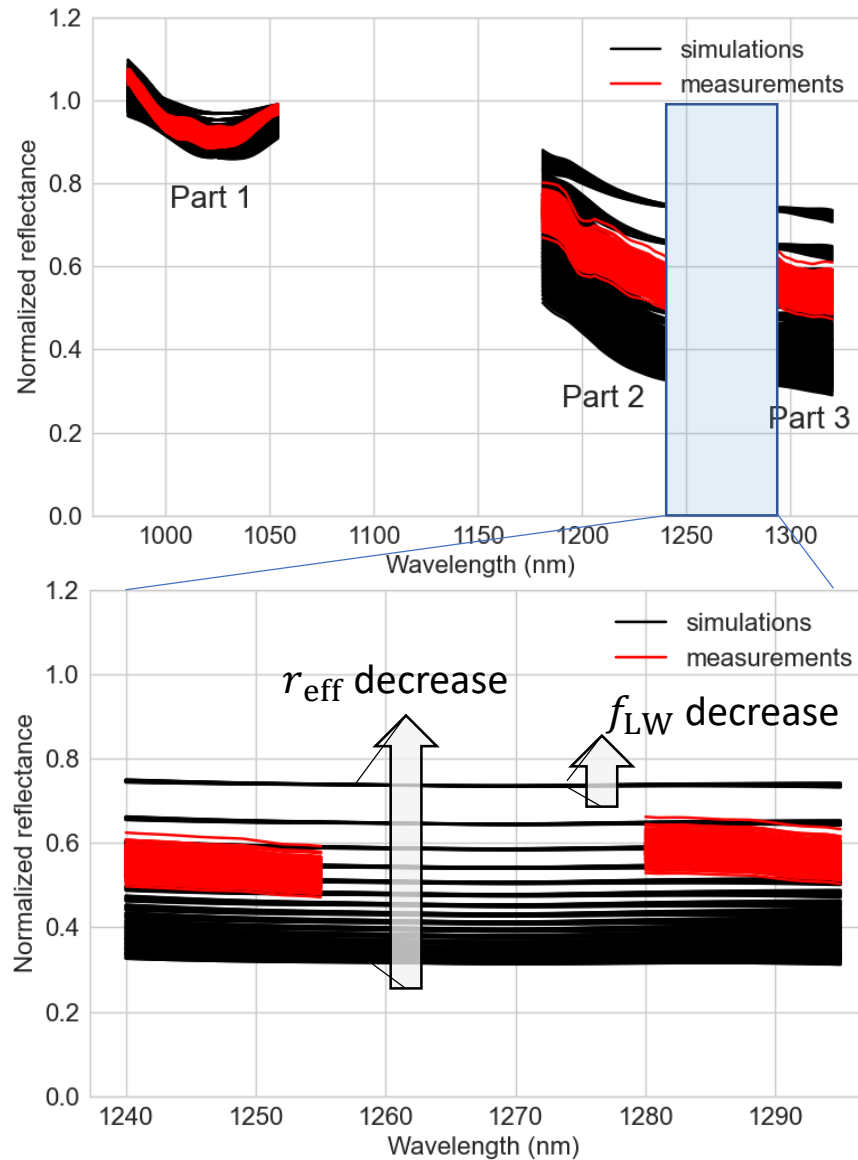


Retrieval of f_{LW} (Part 1) and r_{eff} (Part 1-3)

Retrieval of snow layer properties

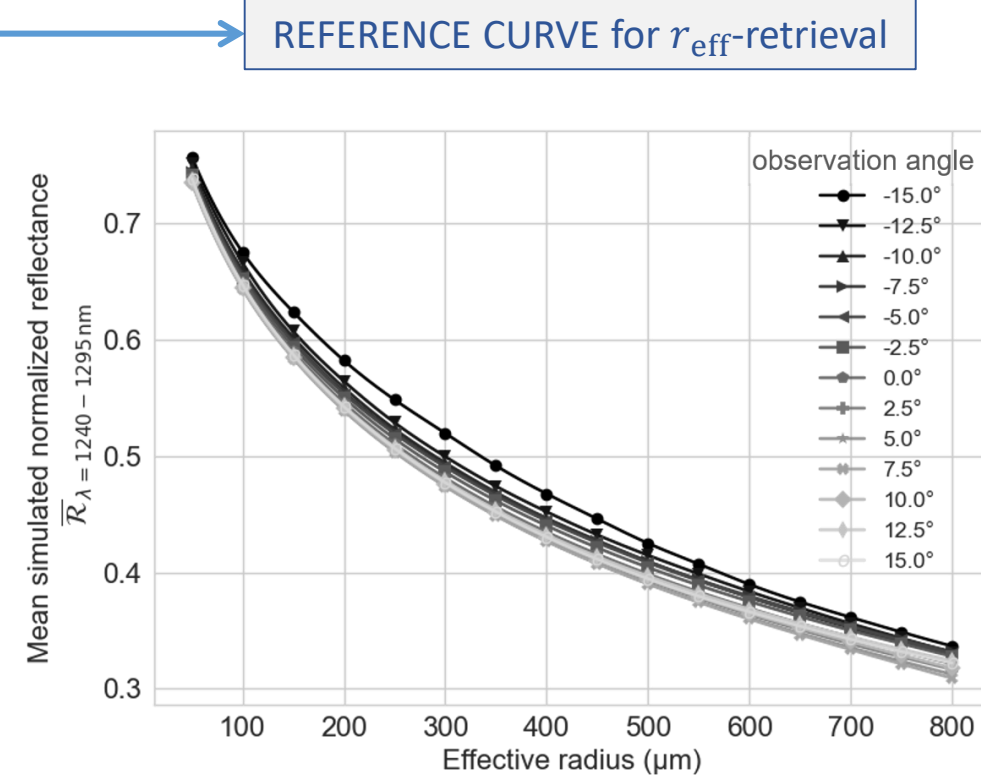
APPROACH →

spectral independence of f_{LW}



Avgaging over
all f_{LW} and
wavelength interval

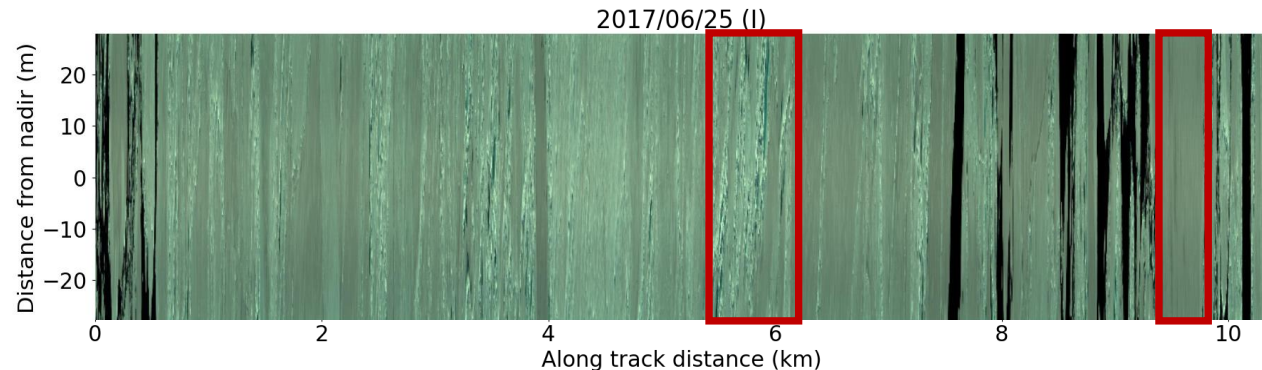
$\lambda = 1240 - 1295 \text{ nm}$
isolated dependence
on r_{eff}



Retrieval of snow layer properties

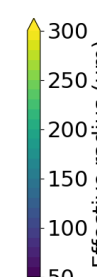
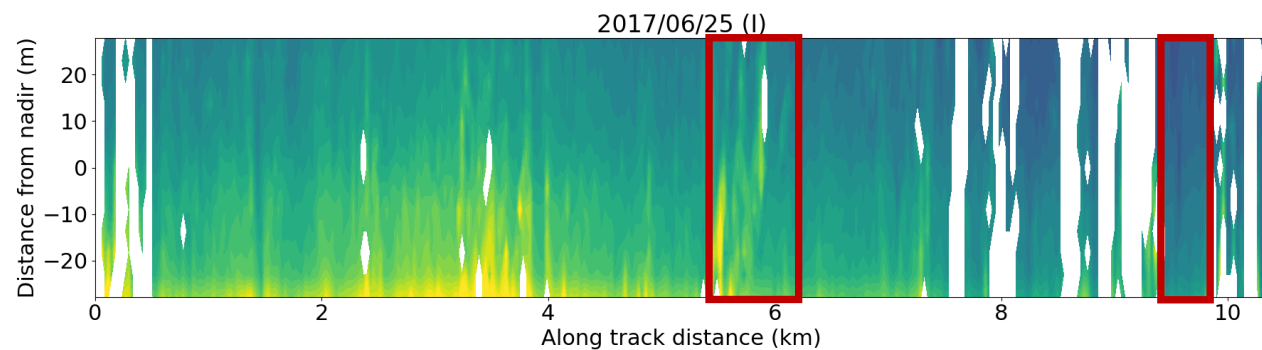
RESULTS

AisaEagle
RGB composite

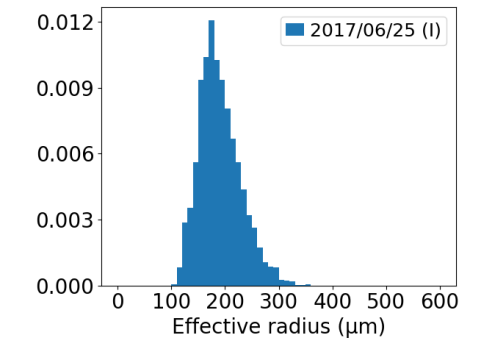


left: pressure ridges and melt ponds
right: homogeneous snow surface

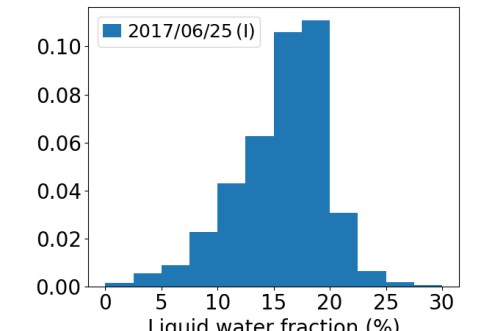
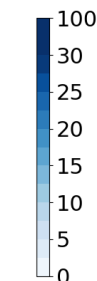
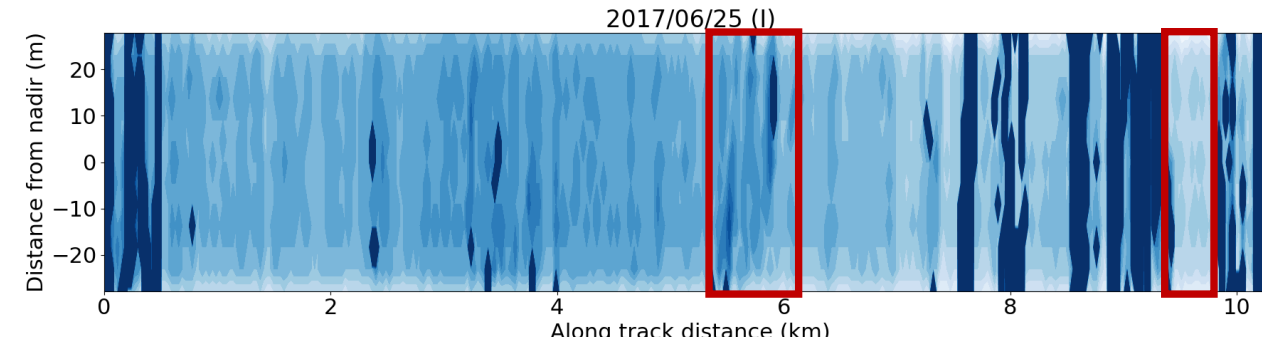
r_{eff} -map

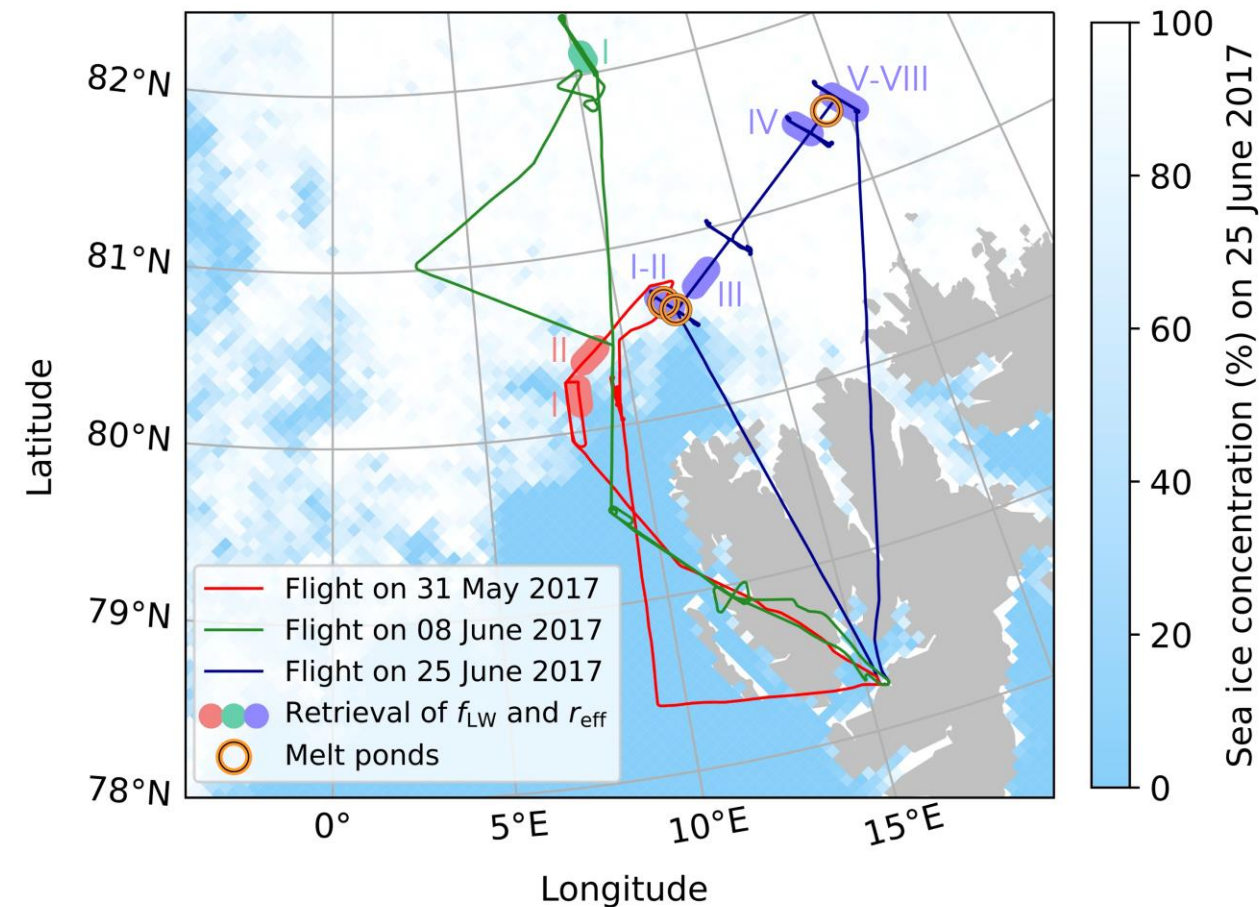


Frequency distribution

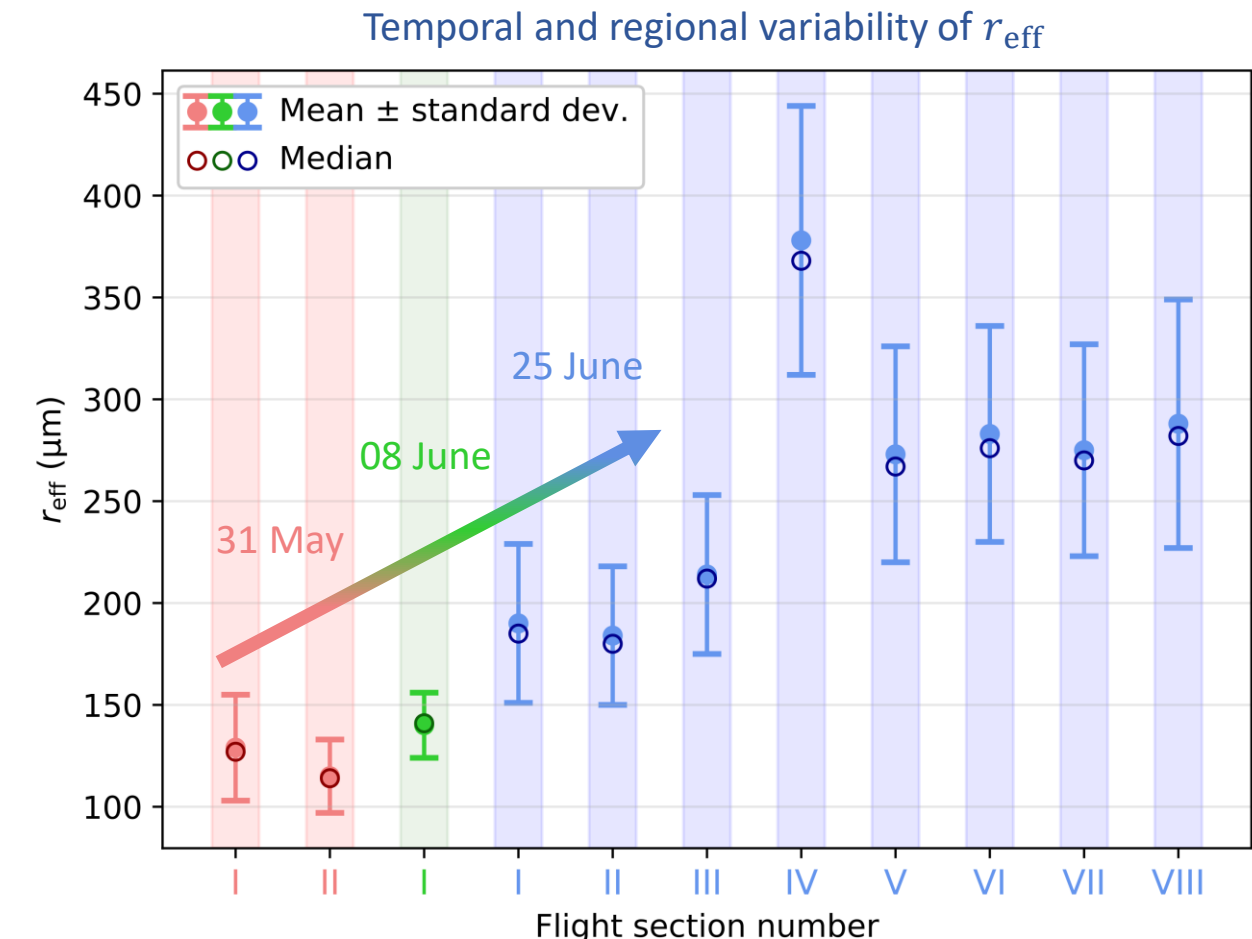


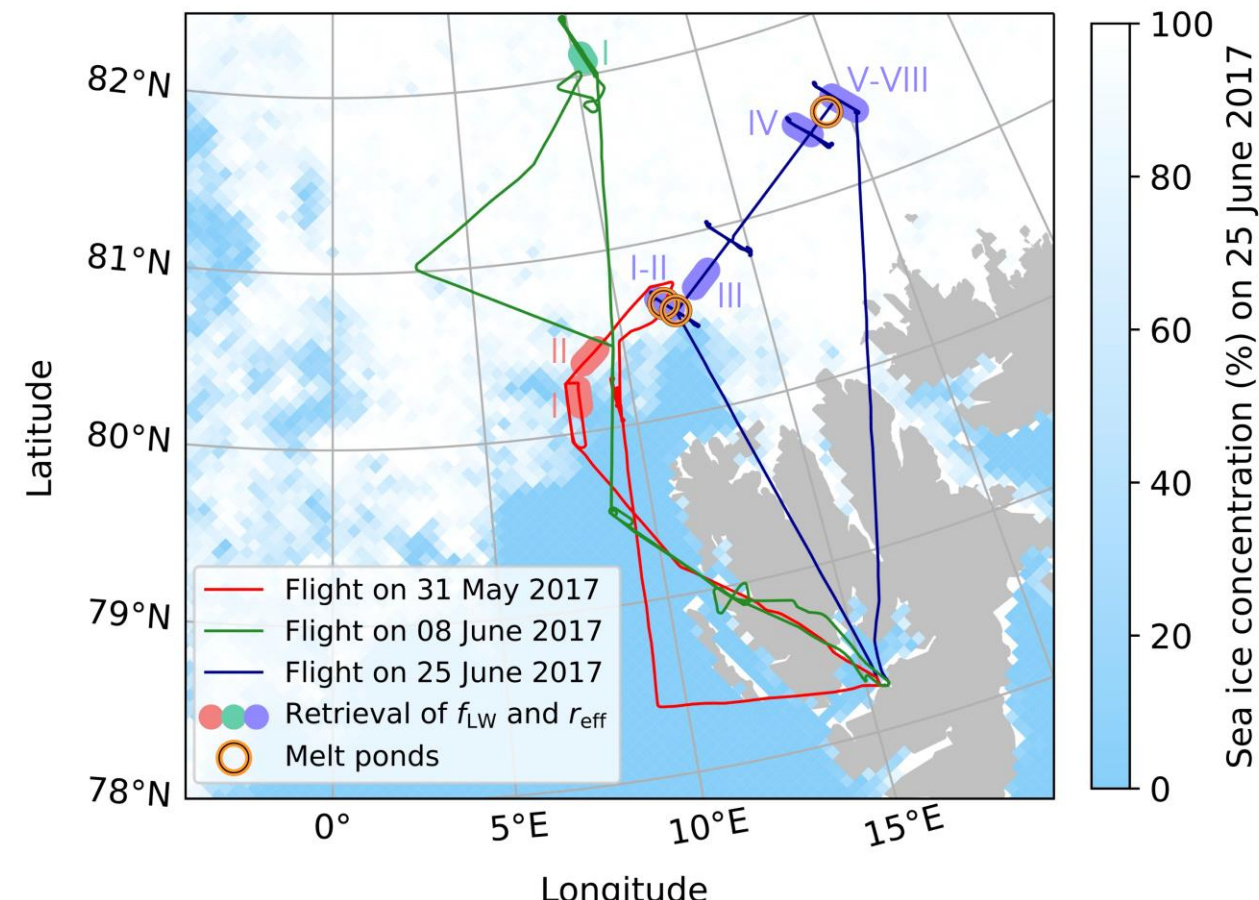
f_{LW} -map





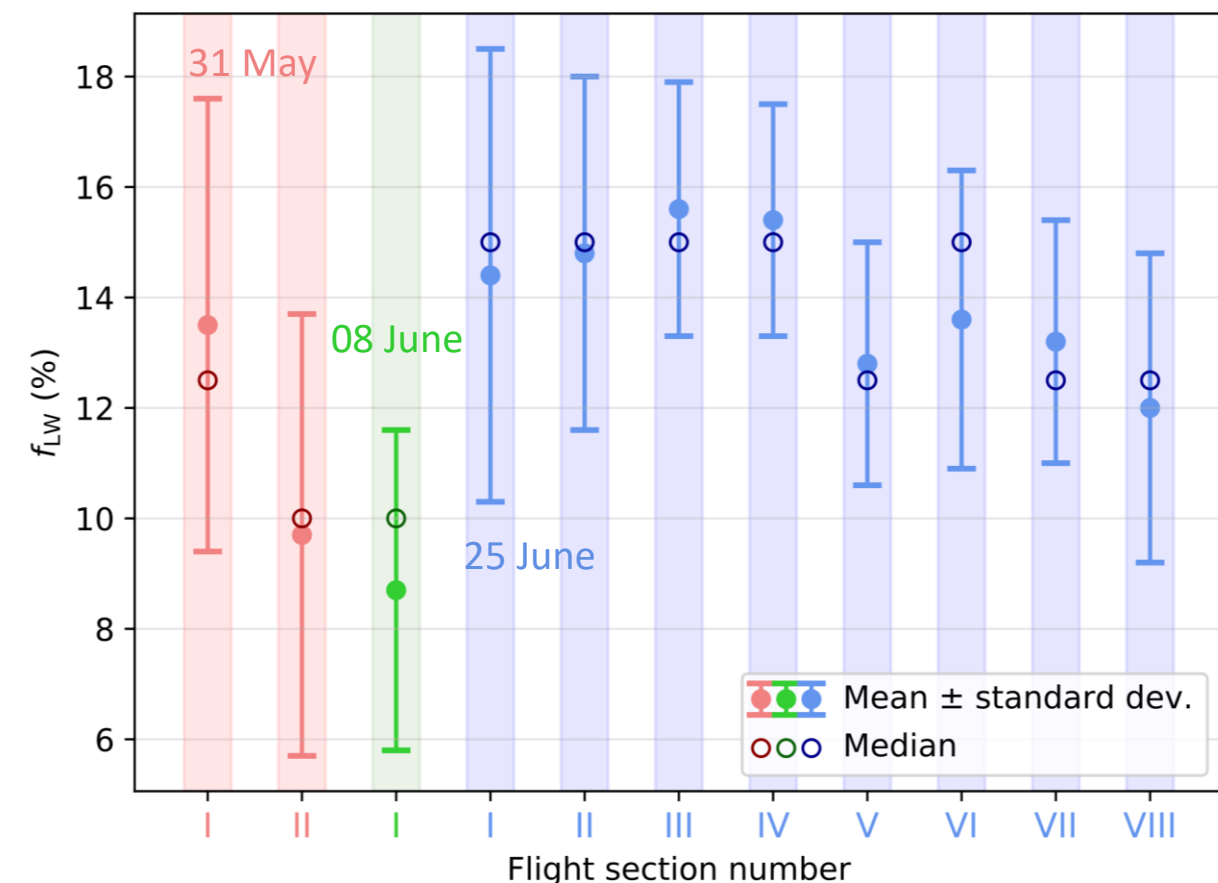
→ Overall, temporally increasing r_{eff} (snow metamorphism) but also local effects!





→ f_{LW} is strongly depending on geographical location

Temporal and regional variability of f_{LW}



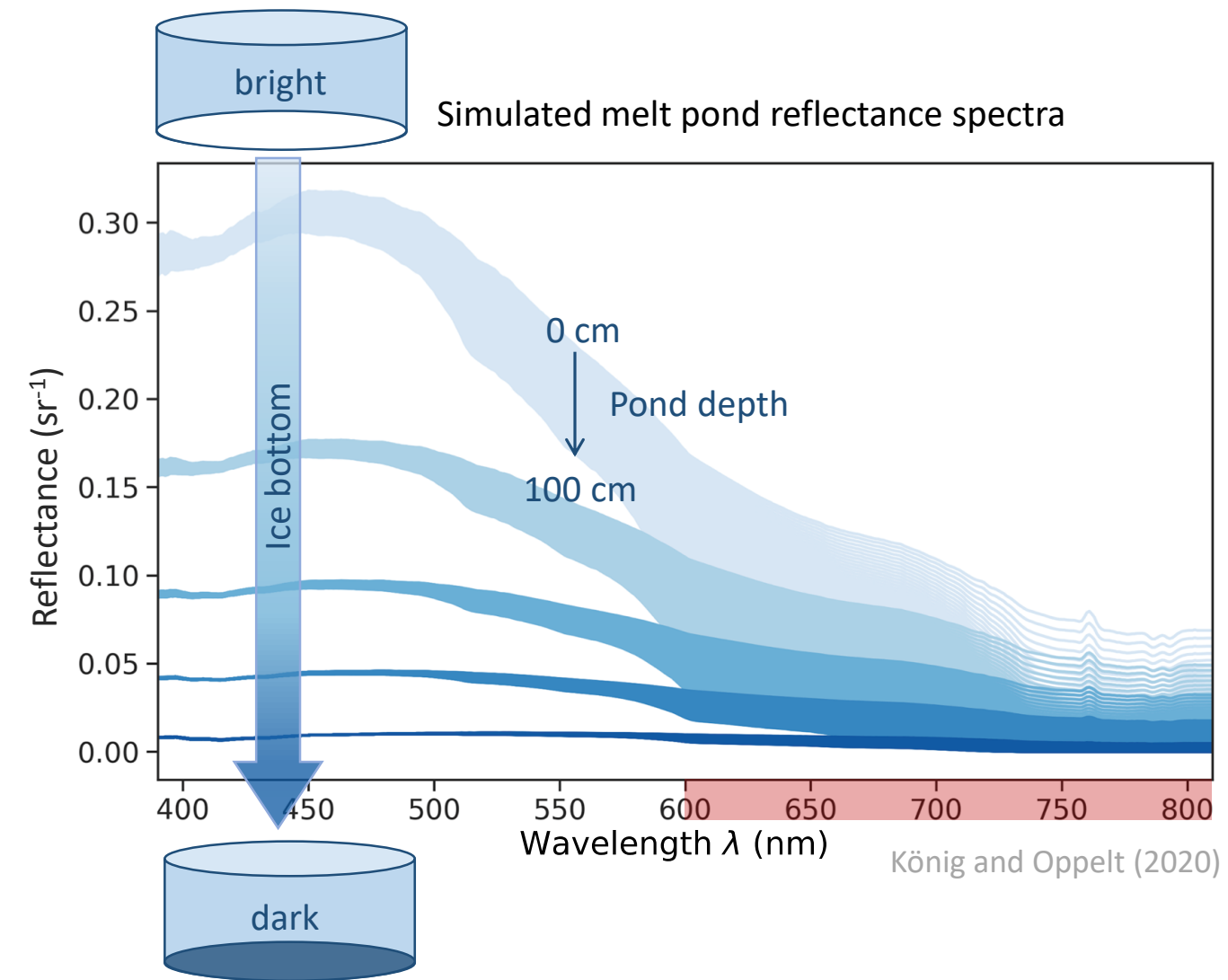
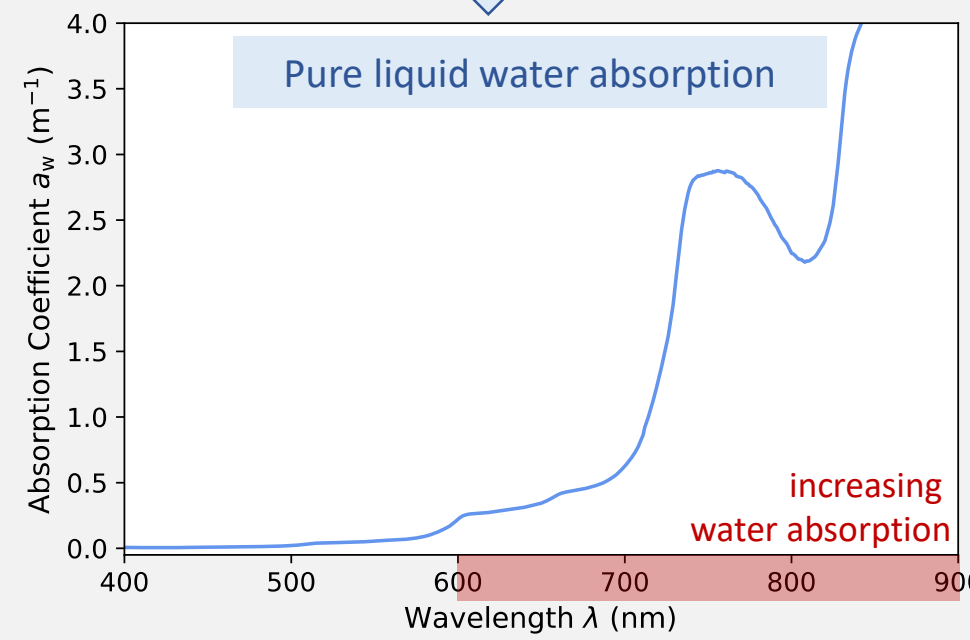
→ masked seasonal effects

THEORY

Melt pond reflectance depending on

→ Ice bottom reflectance

→ Melt pond depth



APPROACH

AIM

Finding reflectance property
widely independent of
the ice bottom reflectance



Linear model
by König and Oppelt (2020)

$$z = a(\theta_{\text{Sun}}) + b(\theta_{\text{Sun}}) \left[\frac{\partial \log(\mathcal{R}_\lambda \cdot \pi^{-1})}{\partial \lambda} \right]_{\lambda=710 \text{ nm}}$$

z Melt pond depth
 θ_{Sun} Solar zenith angle

Slope of log-scaled
reflectance spectrum
at $\lambda = 710 \text{ nm}$

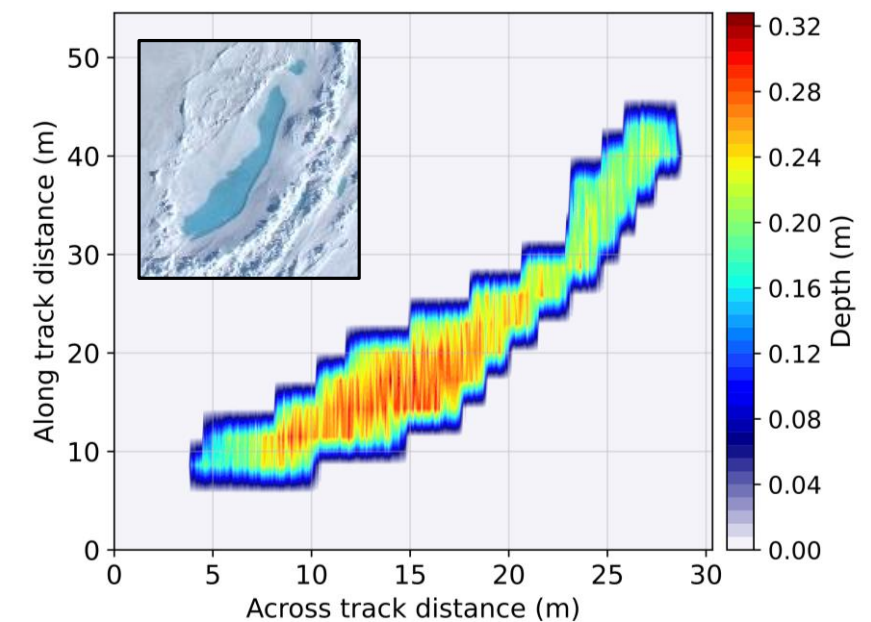
APPLICATION

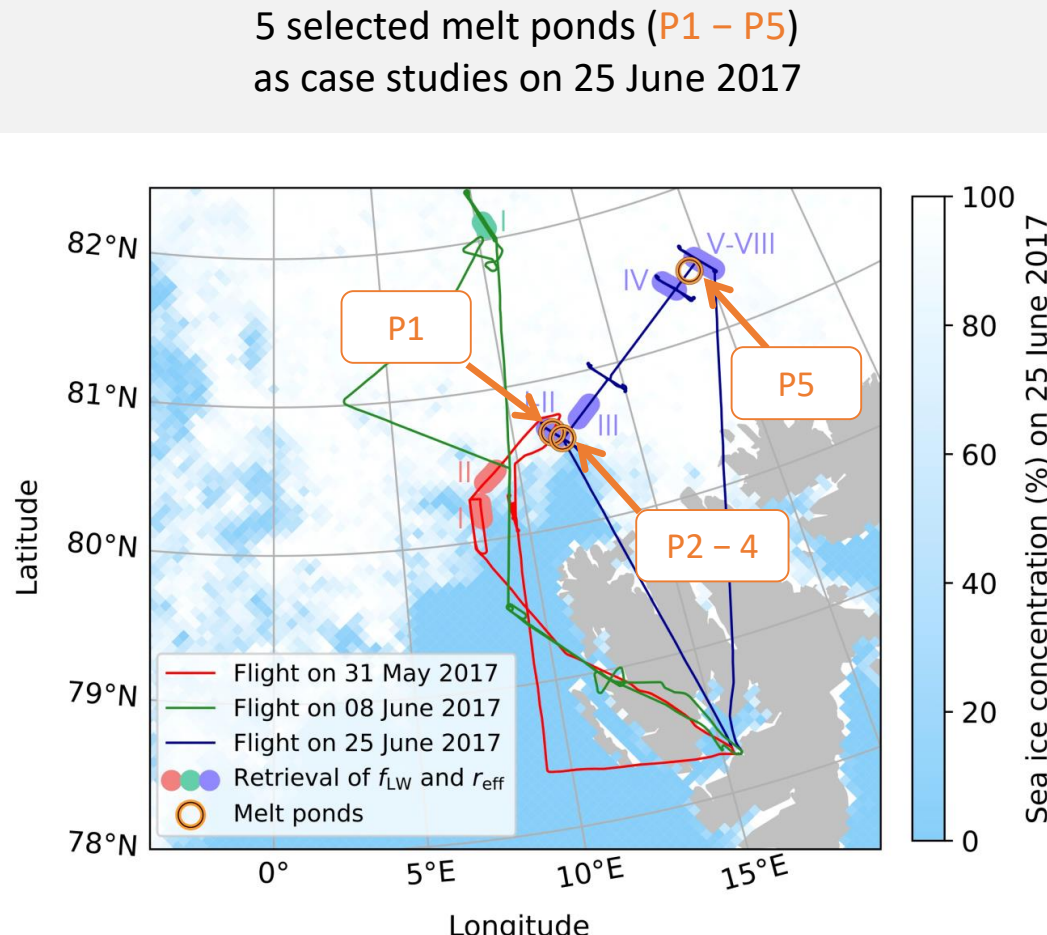
Assumptions/Limitations

- Cloud-free conditions
- Pure pond water
- No water surface reflections
- Complete independence of ice bottom reflectance

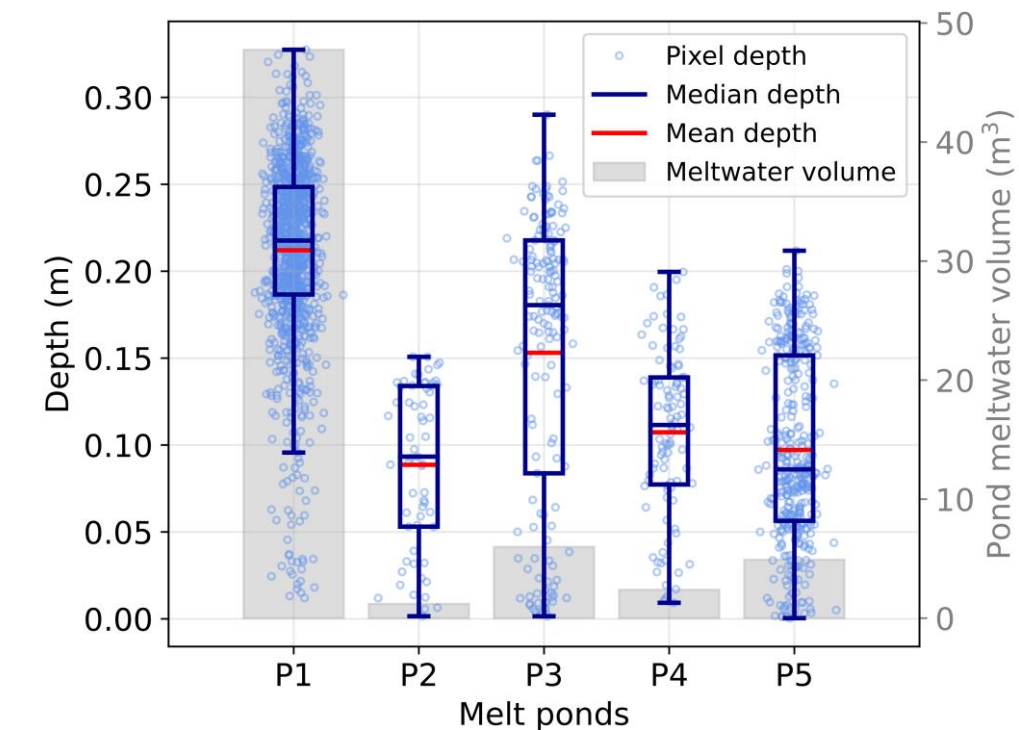
RESULT

Retrieved depth
for each detected
melt pond pixel





Depth distribution and meltwater volume



Melt pond depth

in-pond and spatial variability depending on

sea ice surface topography

meltwater availability

Potential uncertainty sources



No ground-based reference measurements available

Retrieval of snow layer properties

AisaHawk, SMART

Temporal averaging
(aircraft heading/altitude,
solar azimuth/zenith angle)

Realistic reflective behavior of snow layer
in radiative transfer simulations?

$$\begin{aligned} r_{\text{eff}} &\longrightarrow \pm 70 \mu\text{m} \\ f_{\text{LW}} &\longrightarrow \pm 18 \% \end{aligned}$$

Main uncertainty sources

Measurement uncertainties

Data processing

Approach

Maximum uncertainty

Retrieval of melt pond depth

AisaEagle, SMART

Spectral smoothing,
reflectance slope calculation

Linear model RMSE = 0.03 m

$$z \longrightarrow \pm 0.1 \text{ m}$$

CONCLUSION

Potential of airborne spectral imaging
to map melting processes on Arctic sea ice



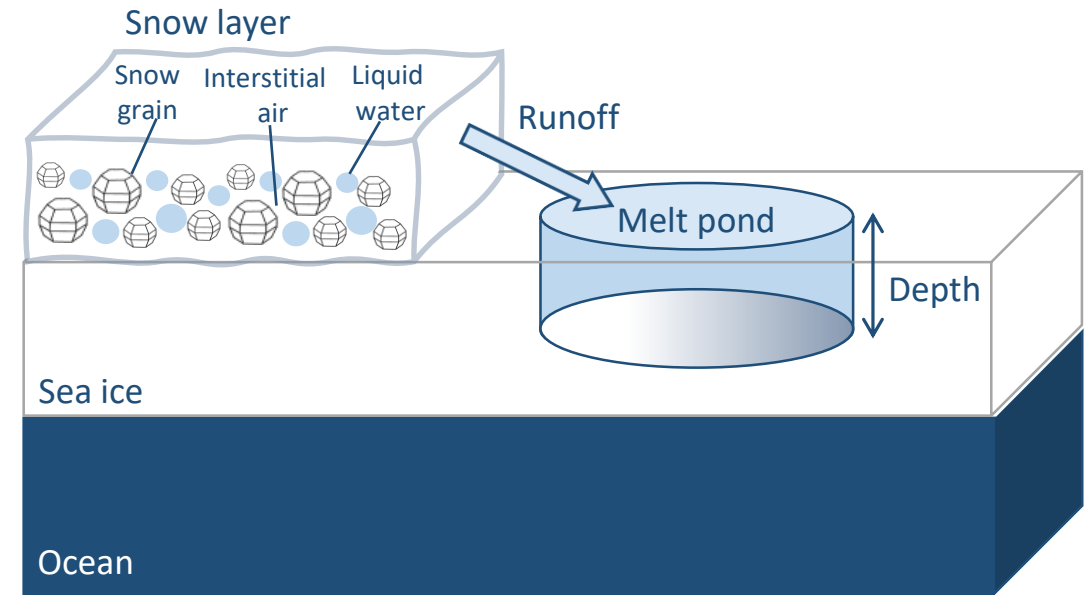
Further improvement

- Reference measurements for validation
- Spatially and temporally expanded measurements to map seasonal development

Further information

Manuscript submitted to AMT, other studies

I. SNOW MELTING II. PONDING



MEASUREMENTS

Wendisch et al. (2019)



Ehrlich et al. (2019)



Wesche et al. (2016)



SIMULATIONS

Yang et al. (2000)



Emde et al. (2016)



Mayer et al. (2019)



APPROACHES

Green et al. (2002)



Donahue et al. (2022)



König and Oppelt (2020)

